Mechanism of Scavenging Action of *N*-Acetylcysteine for the OH Radical: A Quantum Computational Study

Neha Agnihotri and P. C. Mishra*

Department of Physics, Banaras Hindu University, Varanasi - 221 005, India

Received: April 20, 2009; Revised Manuscript Received: July 15, 2009

N-Acetylcysteine, a precursor of glutathione, is an effective antioxidant present in biological systems. The mechanism of scavenging action of *N*-acetylcysteine for the OH radical was studied theoretically. For this purpose, reactions of the OH radical at the different sites of *N*-acetylcysteine were investigated. All the relevant extrema on the potential energy surfaces were located by optimizing the geometries of the reactant and product complexes as well as those of the transition states at the BHandHLYP/AUG-cc-pVDZ level of density functional theory in the gas phase. The solvent effect of aqueous media was treated by performing single point energy calculations at the BHandHLYP/AUG-cc-pVDZ and MP2/AUG-cc-pVDZ levels of theory employing the polarizable continuum model. Correction for basis set superposition error (BSSE) was made by the counterpoise method. Rate constants for all the reaction mechanisms were calculated including the tunneling contributions. Our calculations show that the hydrogen atom of the SH group of *N*-acetylcysteine would be most efficiently abstracted by the OH group, which is in agreement with experimental observations.

1. Introduction

To prevent the various mutation-related diseases, e.g., cancer and Alzemieher's and Parkinson's diseases, exposure to risk factors should be minimized.[1] These factors include reactive oxygen species, reactive nitrogen oxide species, and alkylating agents that are generated in biological environments. These species react with DNA, modify the same, and thus cause mutation. Some common reactive oxygen species and reactive nitrogen oxide species are the superoxide radical anion ($O_2^{\bullet -}$), hydroxyl radical ($OH^{\bullet}$), peroxyl radical ($RO_2^{\bullet}$), alkoxyl radical ($RO^{\bullet}$) (R = alkyl group), HOCl, H_2O_2, H_2O_3, peroxynitrite ($ONOO^-$), $NO^{\bullet}$, $NO_2^{\bullet}$, etc.[2] Among all the reactive oxygen species, the hydroxyl radical is most common and most reactive. It can be generated from hydrogen peroxide in the presence of ferrous ions by the Fenton reaction.[3] It can react with almost all biomolecules leading to DNA strand break,[3−5] DNA−protein cross-link,[6] base-pair mutation,[7,8] base oxidation,[9,10] lipid peroxidation,[11] and other damaging effects.[12] Therefore, it is very necessary to scavenge it from cells to protect them from its oxidative action. Fortunately, there are chemical species present in biological environments that scavenge it efficiently.

Antioxidants are the substances that protect biological systems from oxidizing agents. They may act by different mechanisms including transformation of the oxidizing agents into nondamaging forms.[13,14] They decrease oxidative stress on biological systems by scavenging reactive oxygen species or reactive nitrogen oxide species.[14,15] The most common antioxidants present in biological systems are *N*-acetylcysteine (NAC) (glutathione precursor), β-carotene (vitamin A precursor), ascorbic acid (vitamin C), α-tocopherol (vitamin E), uric acid, urocanic acid, etc.[15−19] Internal antioxidant production declines with aging, increasing the risk for various diseases. It makes oral ingestion of nutritional antioxidants very important.

Glutathione is the most important scavenger of reactive oxygen species and a major detoxifying agent inside our body, particularly in the brain. Reduced glutathione (GSH) plays a central physiological role in protecting cells against exogenous and endogenous oxidants, toxicants, DNA damaging agents, and carcinogens.[20,21] Glutathione is produced inside cells and cannot be ingested as a supplement as it is too large a molecule to pass through the intestinal walls. It is produced in biological systems from the amino acids cysteine, glutamic acid, and glycine. Glutathione levels cannot be increased by ingesting cysteine orally because oral cysteine is potentially toxic and is spontaneously destroyed in the gastronomical tract.[22] However, NAC can be ingested orally, is the bioavailable form of cysteine, and acts as a precursor for glutathione synthesis.[23−27]

NAC is more water-soluble than cysteine and is a weak acid with a pK_a value of 2 for the acidic group and 9.5 for the thiol group.[28] It acts as an excellent scavenger of the OH radical with

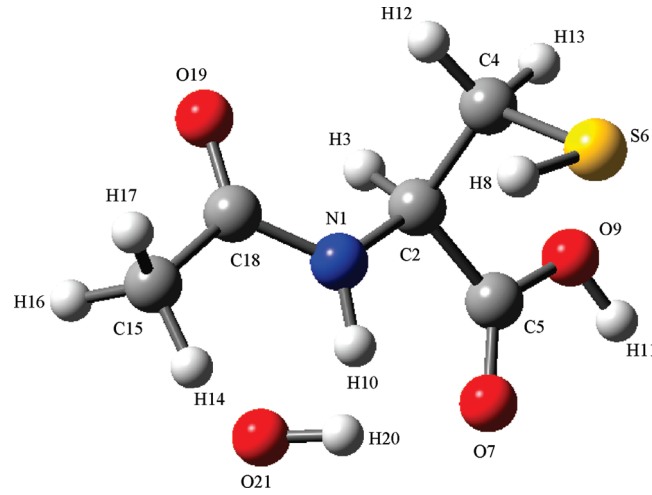

Figure 1. Structure of the complex of the most stable conformer of NAC ($C_5H_9NO_3S$) with an OH group obtained at the BHandHLYP/AUG-cc-pVDZ level of theory in the gas phase. The adopted atomic numbering scheme is also shown.

* Corresponding author. E-mail address: pcmishra_in@yahoo.com.

10.1021/jp903604s CCC: $40.75
Published on Web 08/06/2009

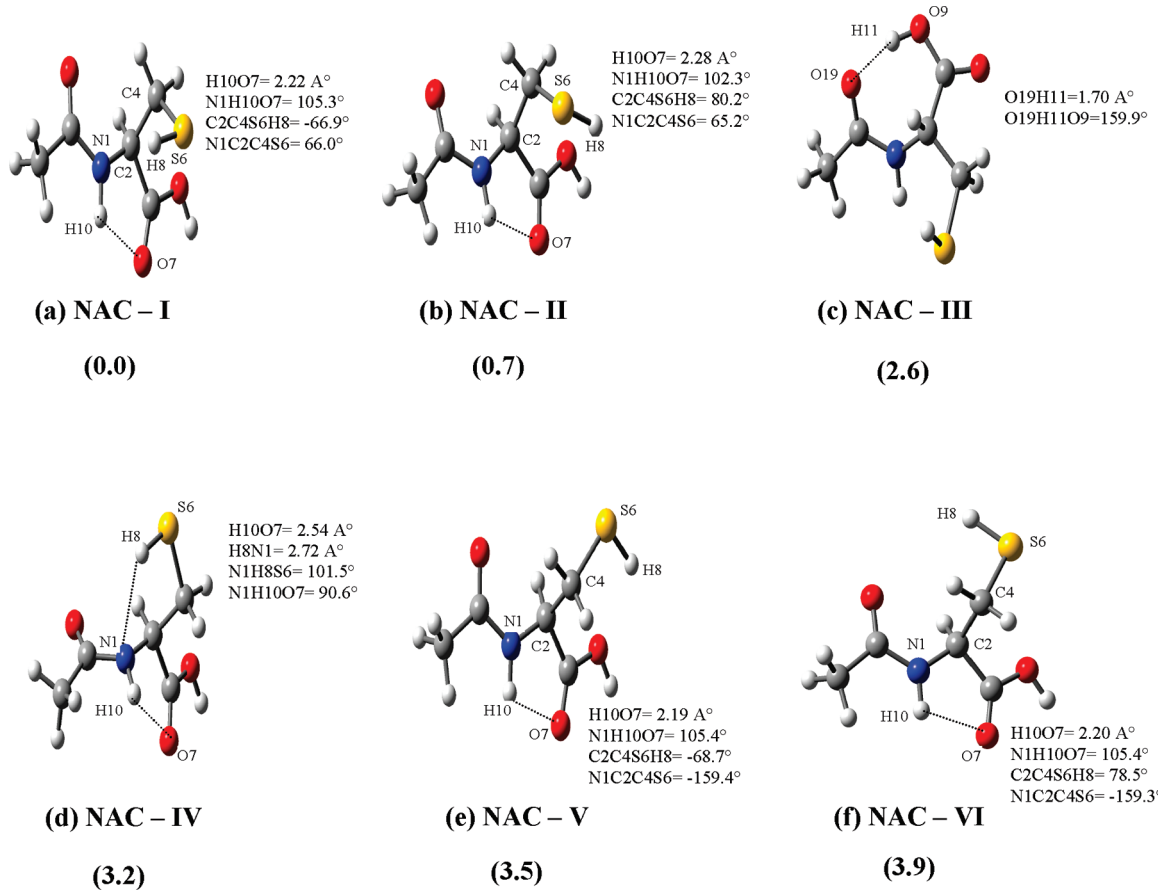

Figure 2. Structures of six lowest-energy conformers (a−f) of *N*-acetylcysteine. Relative ZPE-corrected total energies (kcal/mol) of the six conformers (a−f) obtained at the MP2/AUG-cc-pVDZ level of theory in aqueous media are given with respect to that of (a).

TABLE 1: Relative ZPE-Corrected Total Energies (ΔE_i) and Corresponding Gibbs Free Energy Changes (ΔG_i) (i = a−f) at 298.15 K (kcal/mol) of Six Lowest-Energy Conformers of *N*-Acetylcysteine (NAC-I to NAC-VI) Obtained at Different Levels of Theory in the Gas Phase and Aqueous Media with Respect to Those of the Most Stable Conformer (NAC-I)

		gas phase		aqueous media	
conformers	relative ZPE-corrected and Gibbs free energies	BHandHLYP/ AUG-cc-pVDZ	MP2/ AUG-cc-pVDZ	BHandHLYP/ AUG-cc-pVDZ	MP2/ AUG-cc-pVDZ
NAC-I	ΔE_a	0.0	0.0	0.0	0.0
	ΔG_a	0.0	0.0	0.0	0.0
NAC-II	ΔE_b	0.5	0.5	0.7	0.7
	ΔG_b	0.2	0.2	0.4	0.4
NAC-III	ΔE_c	1.5	1.6	2.8	2.6
	ΔG_c	2.0	2.2	3.4	3.2
NAC-IV	ΔE_d	2.5	3.0	2.4	3.2
	ΔG_d	1.9	2.4	1.8	2.6
NAC-V	ΔE_e	2.3	2.9	3.3	3.5
	ΔG_e	2.0	2.6	3.1	3.3
NAC-VI	ΔE_f	2.9	3.3	3.8	3.9
	ΔE_f	2.1	2.7	3.1	3.3

the rate constant 1.36×10^{10} M^{-1} s^{-1} observed in pulse radiolysis experiments.[29] The reaction for its scavenging action can be described as[29]

$$C_5H_8NO_3SH + OH^{\bullet} \rightarrow C_5H_8NO_3S^{\bullet} + H_2O$$

The antioxidant property of NAC arises due to its thiol group.[30] Many thiol group containing molecules have antioxidant property, have potential to inactivate reactive oxygen species, and are used in the treatment of chronic inflammatory and respiratory diseases.[31] NAC can be considered as a powerful antioxidant and a potent cancer preventive agent as it protects cells from extracellular mutagenic agents from exogenous and endogenous sources.[31,32] Thus NAC neutralizes reactive oxygen species, inhibits their genotoxicity, protects DNA and nuclear enzymes from them, and prevents the formation of carcinogen−DNA adducts.[1,21,23−27,32] NAC in cells can be detected by different experimental methods.[33,34] Several studies have been performed to evaluate the ability of various antioxidants including NAC to protect cells from reactive oxygen species and reactive nitrogen oxide species.[13] However, to the best of our knowledge, there is no theoretical study reported so far regarding the scavenging action of NAC toward these species. Here, we have studied the reaction mechanism involved in the scavenging action of NAC toward the OH radical.[12]

TABLE 2: ZPE-Corrected Barrier Energies (ΔE_i^b) and Corresponding Gibbs Free Energy Barriers (ΔG_i^b) ($i = 1-6$) at 298.15 K (kcal/mol) Involved in the Hydrogen Abstraction Reactions by an OH Radical from the Different Sites of NAC According to Schemes 1−6 in the Gas Phase

		without BSSE correction			with BSSE correction	
active sites for the reaction	relative barrier energies	B3LYP/ AUG-cc-pVDZ	BHandHLYP/ AUG-cc-pVDZ	MP2/ AUG-cc-pVDZ	BHandHLYP/ AUG-cc-pVDZ	MP2/ AUG-cc-pVDZ
N1	ΔE_1^b	3.0	14.6	10.4	15.3	10.8
	ΔG_1^b	4.5	16.3	12.0	16.9	12.5
S6	ΔE_2^b	3.0	1.9	0.7	2.3	0.9
	ΔG_2^b	3.2	3.2	2.0	3.6	2.2
O9	ΔE_3^b	0.8	14.6	16.4	14.9	16.7
	ΔG_3^b	1.3	15.8	17.7	16.1	17.9
C2	ΔE_4^b	–0.1	5.8	3.9	5.7	4.2
	ΔG_4^b	2.2	7.1	5.2	7.0	5.5
C4	ΔE_5^b	7.2	7.8	6.7	8.2	7.0
	ΔG_5^b	7.9	8.9	7.8	9.3	8.2
C15	ΔE_6^b	3.5	12.0	9.2	12.4	9.6
	ΔG_6^b	4.3	13.2	10.5	13.7	10.8

TABLE 3: ZPE-Corrected Barrier Energies (ΔE_i^b) and Corresponding Gibbs Free Energy Barriers (ΔG_i^b) ($i = 1-6$) at 298.15 K (kcal/mol) Involved in the Hydrogen Abstraction Reactions by an OH Radical from the Different Sites of NAC According to Schemes 1−6 in Aqueous Media

		without BSSE correction			with BSSE correction	
active sites for the reaction	relative barrier energies	B3LYP/ AUG-cc-pVDZ	BHandHLYP/ AUG-cc-pVDZ	MP2/ AUG-cc-pVDZ	BHandHLYP/ AUG-cc-pVDZ	MP2/ AUG-cc-pVDZ
N1	ΔE_1^b	3.9	14.1	10.4	15.7	11.1
	ΔG_1^b	5.4	15.8	12.0	17.4	12.8
S6	ΔE_2^b	2.9	–0.6	–0.7	–0.9	–0.3
	ΔG_2^b	3.1	0.7	0.6	0.4	1.0
O9	ΔE_3^b	1.8	11.2	10.1	11.4	11.0
	ΔG_3^b	2.2	12.4	11.3	12.6	12.2
C2	ΔE_4^b	–1.3	5.9	4.5	6.3	5.4
	ΔG_4^b	1.1	7.2	5.8	7.6	6.7
C4	ΔE_5^b	8.1	9.4	9.2	9.9	9.1
	ΔG_5^b	8.9	10.5	10.3	11.0	10.2
C15	ΔE_6^b	–1.0	7.6	4.4	8.0	5.4
	ΔG_6^b	–0.2	8.9	5.7	9.2	6.7

2. Computational Details

To obtain the lowest-energy structure of NAC, some of its conformers based on previous studies on it and cysteine were considered. For this purpose, as discussed in the next subsection, geometries of six conformers of NAC were fully optimized in the gas phase at the BHandHLYP/AUG-cc-pVDZ level of density functional theory (DFT).[35,36] The BHandHLYP functional of DFT was employed here as it has been shown to be reliable, in some cases more reliable than the popular functional B3LYP.[37,38] The results obtained in the present work on reaction barrier energies also support the previous observations in this regard.[37,38] Single-point energy calculations were performed at the MP2/AUG-cc-pVDZ level of theory[39,40] in the gas phase for all the selected conformers of NAC using the geometries optimized at the BHandHLYP/AUG-cc-pVDZ level. To treat the bulk solvent effect, single-point energy calculations at the BHandHLYP/AUG-cc-pVDZ and MP2/AUG-cc-pVDZ levels of theory were carried out using the polarizable continuum model (PCM)[41,42] of the self-consistent reaction field theory employing the geometries optimized at the BHandHLYP/AUG-cc-pVDZ level in the gas phase.

Geometries of all the reactant and product complexes as well as those of the transition states involved in the reactions of the hydroxyl radical at the different sites of NAC were optimized in the gas phase using the B3LYP and BHandHLYP functionals of DFT along with the AUG-cc-pVDZ basis set. Single-point energy calculations at the MP2/AUG-cc-pVDZ level of theory in the gas phase were carried out using the geometries optimized at the BHandHLYP/AUG-cc-pVDZ level. Solvation in aqueous media was treated by single-point energy calculations at the B3LYP/AUG-cc-pVDZ level using the PCM and employing the geometries optimized at the same level of theory in the gas phase. Solvation in aqueous media was also treated by single-point energy calculations at the BHandHLYP/AUG-cc-pVDZ and MP2/AUG-cc-pVDZ levels of theory using the PCM employing the geometries optimized at the BHandHLYP/AUG-cc-pVDZ level of theory in gas phase.

The genuineness of the calculated transition states was confirmed by visually examining the vibrational modes related to the imaginary frequencies and applying the condition that these connected the corresponding reactant and product complexes properly. Since the transition states were located fully convincingly, intrinsic reaction coordinate (IRC) calculations in this regard were not required.[43] Correction for basis set superposition error (BSSE) was made by single-point energy calculations in the gas phase and aqueous media at the BHandHLYP/AUG-cc-pVDZ level of theory using the counterpoise method.[44,45] The BSSE corrections obtained at the BHandHLYP/AUG-cc-pVDZ level were also applied to the total energies obtained at the MP2/AUG-cc-pVDZ level. Electron and spin density distributions were studied in the reactant and product complexes as well as the transition states at the BHandHLYP/AUG-cc-pVDZ level of theory in the gas phase. All the calculations were performed employing the Windows versions of the Gaussian98 (G98W)[46] and Gaussian03 (G03W)[47] suites of programs. For visualization of optimized structures and vibrational modes, the GaussView program[48] was employed.

TABLE 4: Reaction Rate Constants K_i ($i = 1-6$) in L m^{-1} s^{-1} at 298.15 K for the Abstraction Reactions of Hydrogen Atoms by an OH Radical from the Different Sites of NAC (Schemes 1−6) in the Gas Phase and Aqueous Media Obtained Using BSSE-Corrected Gibbs Free Energies

Reaction	Rate constant($Lm^{-1}s^{-1}$)			
	BHandHLYP/AUG-cc-pVDZ		MP2/AUG-cc-pVDZ	
	Gas phase	Aqueous media	Gas phase	Aq. med.
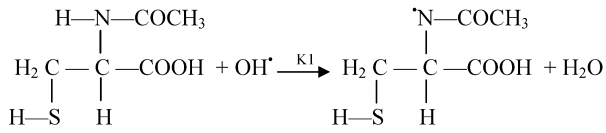	0.64×10^2	0.28×10^2	1.09×10^5	6.56×10^4
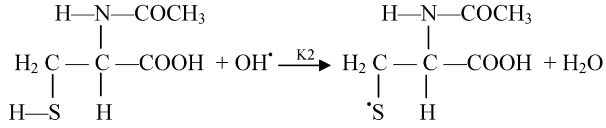	3.24×10^{11}	7.20×10^{13}	3.45×10^{12}	2.62×10^{13}
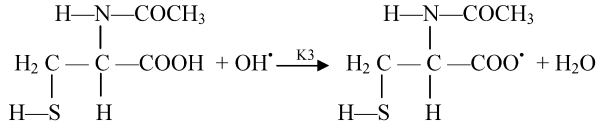	2.37×10^2	8.71×10^4	0.11×10^2	1.71×10^5
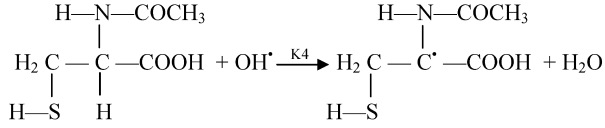	1.09×10^9	3.97×10^8	1.38×10^{10}	1.82×10^9
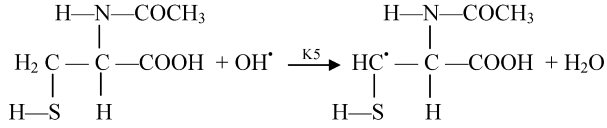	2.22×10^7	1.25×10^6	1.42×10^8	4.83×10^6
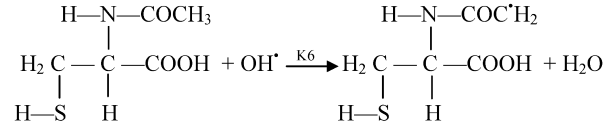	1.38×10^4	2.74×10^7	1.84×10^6	1.87×10^9

Rate constants $k(T)$ of reactions can be obtained using the formula[49−52]

$$k(T) = \Gamma(T)\frac{k_B T}{h} V_m^{(n-1)} e^{-\Delta G/RT}$$

where $\Gamma(T)$ is the tunneling factor; k_B is Boltzmann's constant; T is the absolute temperature; h is Planck's constant; V_m is molar volume; n is molarity of the reaction; ΔG is the Gibbs free barrier energy; and R is the gas constant. The tunneling factor $\Gamma(T)$ can be obtained approximately using the Wigner transmission coefficient $k^W(T)$ given by[51−53]

$$k^W(T) = 1 + \frac{1}{24}\left[\frac{\hbar\nu}{k_B T}\right]^2$$

where ν is the imaginary frequency of the transition state under consideration.

3. Results and Discussion

3.1. Conformers of NAC. The atomic numbering scheme in a complex of NAC with an OH group, adopted here, is shown in Figure 1. A comprehensive conformational analysis of NAC was not the aim of the present study. However, to obtain its lowest-energy structure, some of its most stable conformers were considered. Six conformers of NAC shown in Figure 2 were optimized at the BHandHLYP/AUG-cc-pVDZ level of theory in the gas phase. Bieri and Burgi[54] have reported a structure of NAC that was optimized at the B3PW91/6-31G level in the gas phase and in aqueous media using the PCM, and that was considered to be the lowest-energy conformer by these authors. However, our study revealed that the conformer reported by these authors[54] is not the most stable one. Instead, we found that the conformer reported by these authors[54] is the second most stable conformer of NAC (NAC-II). The most stable conformer NAC-I differs from NAC-II with respect to the C2C4S6H8 dihedral angle, which has the values −66.9° and 80.2° in the two conformers, respectively.

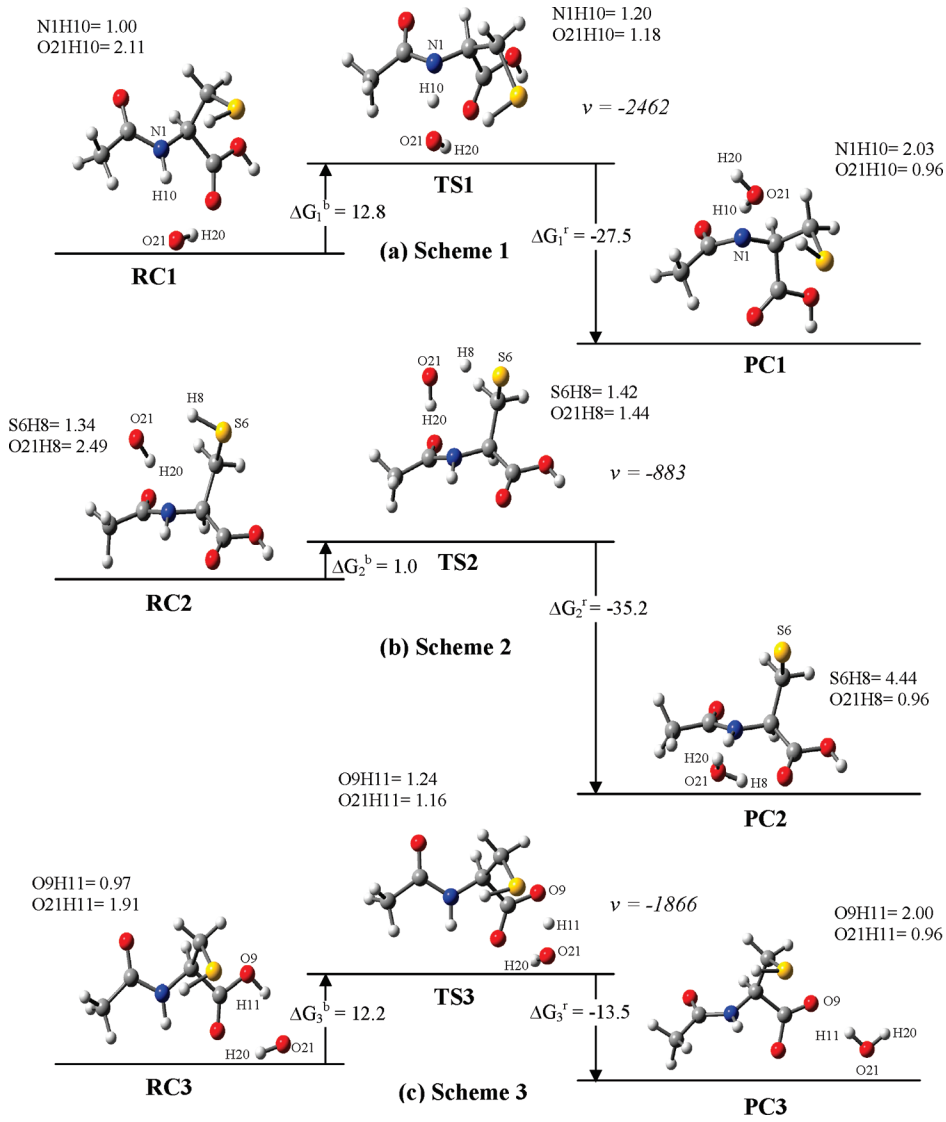

Figure 3. Gibbs free energy barriers (ΔG_n^{b}) and released (ΔG_n^{r}) energies (n = 1, 2, 3) at 298.15 K involved in the hydrogen abstraction reaction by an OH radical from the different sites of NAC obtained at the MP2/AUG-cc-pvDZ level of theory along with BSSE correction in aqueous media. The imaginary vibrational frequencies (ν) associated with all the TSs are given in cm^{-1}. Certain optimized interatomic distances (Å) are also given. The locations of the different structures in terms of energy values are not to scale.

A number of theoretical studies have been performed on conformational analysis of cysteine. Dobrowolski et al.[55] found 51 stable conformers of cysteine in the gas phase. A few of the most stable conformers of cysteine have also been studied in our laboratory[56] from the points of view of stability, normal (nonzwitterionic) to zwitterionic form conversion, and vibrational spectra. We considered the lowest-energy three conformers of cysteine reported in these studies[55,56] and obtained six conformers of NAC by replacing the hydrogen atoms of their amino groups, one at a time, by an acetyl group each. The two most stable conformers of these six conformers of NAC are named as NAC-III and NAC-IV. The other four of the six conformers thus obtained had total energies that were higher than that of NAC-I by about 5 kcal/mol or more each. The conformer NAC-V was obtained by the rotation of the CH_2SH group about the C2C4 bond in NAC-I (Figure 2a). The dihedral angle N1C2C4S6 involved in this rotation is changed by about 90° in going from NAC-I to NAC-V. The sixth most stable conformer (NAC-VI) differs from NAC-V with respect to the dihedral angle C2C4S6H8. In NAC-V and NAC-VI, this dihedral angle was found to be −68.7° and 78.5°, respectively.

ZPE-corrected relative total energies and Gibbs free energies of all the six conformers of NAC obtained at different levels of theory in the gas phase and in aqueous media are presented in Table 1. If we consider the ZPE-corrected total energies obtained by geometry optimization at the BHandHLYP/AUG-cc-pVDZ level followed by single-point energy calculations at the MP2/AUG-cc-pVDZ level in aqueous media, the conformer NAC-I is more stable than the conformers NAC-II, NAC-III, NAC-IV, NAC-V, and NAC-VI by 0.7, 2.6, 3.2, 3.5, and 3.9 kcal/mol, respectively. Thus we find that NAC-I is the most stable conformer of NAC. Further, we note that NAC-I and NAC-II differ in their total energies by less than 1 kcal/mol and would, therefore coexist, the abundance of the former being much more than that of the latter. In the present study, NAC-I was used in the calculations for reactions, but one would expect similar results for reactions involving NAC-II also.

We examined relative stabilities of the normal and zwitterionic structures of NAC. It is known that zwitterionic structures are stabilized in aqueous media.[56,57] The solvent effect of aqueous media includes contributions of both specific water molecules (specific solvent effect) and that of the bulk aqueous

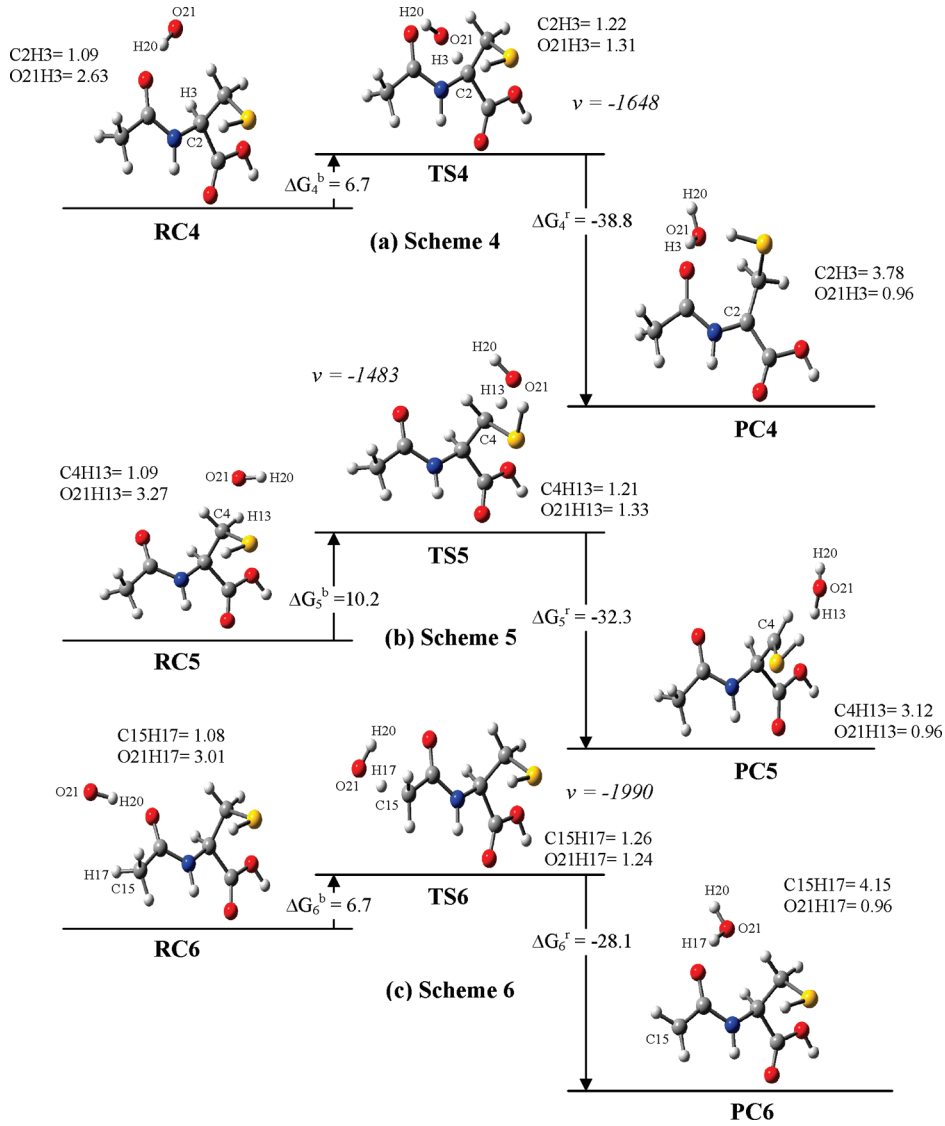

Figure 4. Gibbs free energy barriers (ΔG_n^b) and released (ΔG_n^r) energies ($n = 4, 5, 6$) at 298.15 K involved in the hydrogen abstraction reaction by an OH radical from the different sites of NAC obtained at the MP2/AUG-cc-pVDZ level of theory along with BSSE correction in aqueous media. The imaginary vibrational frequencies (ν) associated with all the TSs are given in cm^{-1}. Certain optimized interatomic distances (Å) are also given. The locations of the different structures in terms of energy values are not to scale.

medium (bulk solvent effect).[56,57] We replaced the hydrogen atoms of the NH_3^+ group of the two most stable conformers of the cysteine zwitterion by an acetyl group each to generate zwitterionic structures of NAC. One specific water molecule was considered to facilitate proton transfer and to take into account the specific solvent effect at the minimal level. The geometries of the complexes of normal and zwitterionic NAC with one water molecule each were optimized in bulk aqueous media at the BHandHLYP/AUG-cc-pVDZ level of theory. The bulk solvent effect was treated using the PCM.[41,42] In the different complexes of zwitterionic NAC with one water molecule each, the optimized NH bond lengths were found to be 1.04−1.08 Å. In normal cysteine, the NH bond lengths of the amino group were found to be ∼1 Å, while in zwitterionic cysteine, the NH bond lengths of the NH_3^+ group were found to be ∼1.03 Å.[56] Thus, in the zwitterionic form of NAC, the NH bond lengths are somewhat elongated in comparison to those in the zwitterionic form of cysteine.

The zwitterionic structures of the complexes of NAC with one water molecule each were found to be stable in aqueous media. However, these complexes were found to be less stable than the most stable complex of NAC-I with one water molecule by 28 kcal/mol or more in aqueous media. These results show that NAC would exist mainly in the normal form in both the gas phase and aqueous media, NAC-I being the most stable conformer. We also studied relative stabilities of complexes of the different conformers of normal NAC with one water molecule each at the BHandHLYP/AUG-cc-pVDZ level by first optimizing geometries of the complexes in the gas phase followed by single-point energy calculations in bulk aqueous media using the PCM.[41,42] In these calculations, the water molecule was placed at four different positions considering hydrogen bonding interactions with each conformer of NAC. A complex of the conformer NAC-I of NAC was found to be most stable. In view of these results, the study of reactions of NAC with an OH radical was performed considering the conformer NAC-I of NAC. Since the most stable structure of NAC (i.e., NAC-I) remains unchanged whether it is isolated or in complexation with a water molecule, we did not include the water molecule in the calculations on reactions.

3.2. Hydrogen Abstraction Reaction Mechanisms. Hydrogen abstraction reactions by an OH radical from the N1, S6,

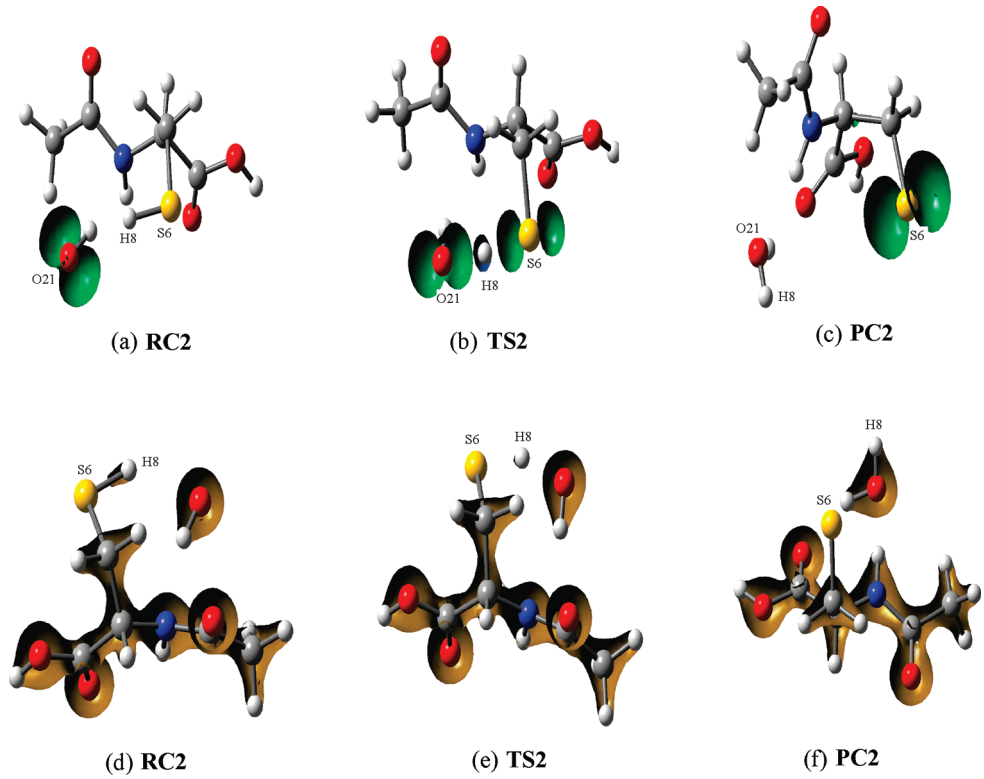

Figure 5. Spin density (a−c) and electron density distributions (d−f) in the reactant complex, transition state, and product complex, respectively, involved in the reaction between NAC and an OH radical shown in scheme 2 (Figure 3b) obtained at the BHandHLYP/AUG-cc-pVDZ level of theory in the gas phase. The surfaces shown in (a−c) correspond to the spin density value 0.01, while those shown in (d−f) correspond to the electron density value 0.2e.

O9, C2, C4, and C15 sites of NAC-I were considered (Figure 1). The calculated ZPE-corrected barrier energies and the corresponding Gibbs free energy changes involved in the reaction of an OH radical at the different sites of NAC-I at the different levels of theory in the gas phase and aqueous media are given in Tables 2 and 3. Reaction rate constants for the different sites calculated using the BSSE-corrected Gibbs free energy changes obtained at the BHandHLYP/AUG-cc-pVDZ and MP2/AUG-ccpVDZ levels in the gas phase and aqueous media are presented in Table 4. The ZPE-corrected barrier energies and corresponding Gibbs free energy changes obtained using the B3LYP functional for the same basis set are usually quite different and significantly less than those obtained using the BHandHLYP functional and the MP2 method. Further, the results obtained using the BHandHLYP functional are usually closer to those obtained by the MP2 method than to those obtained by the B3LYP functional. The MP2 method is expected to be more reliable than the B3LYP functional as electron correlation treatment is superior in the former approach to that in the latter. Thus it seems that the B3LYP functional is less reliable than the BHandHLYP functional in the present context, as noted elsewhere also.[37,38] Due to this reason, BSSE-corrected barrier energies, Gibbs free energy changes, and rate constants were obtained using the BHandHLYP functional and MP2 method only (Tables 2−4).

The reaction shown in scheme 1 (Figure 3a) involves attack of an OH radical on the N1 site of NAC and proceeds from the reactant complex RC1 via the transition state TS1 to the product complex PC1. The BSSE-corrected Gibbs free energy barrier (ΔG_1^b) for scheme 1 at the MP2/AUG-cc-pVDZ level of theory in aqueous media was found to be 12.8 kcal/mol (Table 3). The reaction shown in scheme 2 represents abstraction of the hydrogen atom of the SH group of NAC (Figure 3b) and involves the reactant complex RC2, transition state TS2, and the product complex PC2. In this mechanism, the SH group loses its hydrogen atom to the OH group producing a complex of NAC radical with a water molecule, while the corresponding BSSE-corrected Gibbs free energy barrier (ΔG_2^b) at the MP2/AUG-cc-pVDZ level of theory in aqueous media was found to be 1 kcal/mol (Table 3). The rate constant (K_2) for this reaction step at the MP2/AUG-cc-pVDZ level of theory was found to be 3.45×10^{12} and 2.62×10^{13} L m^{-1} s^{-1} in the gas phase and aqueous media, respectively (Table 4). The experimental value of the rate constant (K_2) in aqueous media is 1.36×10^{10} M^{-1} s^{-1}.[29] Our calculated rate constants in the gas phase and aqueous media are larger than this experimental value by 2 and 3 orders of magnitude, respectively. Nonetheless, theory and experiment agree that the hydrogen atom of the thiol group of NAC would be abstracted most efficiently by an OH group (Table 4).

The reaction shown in scheme 3 (Figure 3c) starts from the reactant complex RC3 and proceeds through the transition state TS3 to the product complex PC3. In this case, the OH group attacks the O9 site of NAC. In RC3, there exists a hydrogen bond between the H atom of the COOH group of NAC and the oxygen atom of the OH group, the hydrogen bond length O21H11 being 1.91 Å. The BSSE-corrected Gibbs free energy barrier for scheme 3 (ΔG_3^b) at the MP2/AUG-cc-pVDZ level of theory in aqueous media was found to be 12.2 kcal/mol (Table 3). The reaction shown in scheme 4 (Figure 4a) represents abstraction of the hydrogen atom attached to the C2 site of NAC. In this mechanism, starting from RC4, the product complex PC4 is formed through the transition state TS4. At TS4, the H3 atom gets detached from the C2 atom and moves toward the O21 atom of the OH group. The BSSE-corrected Gibbs free energy

barrier (ΔG_4^b) in scheme 4 at the MP2/AUG-cc-pVDZ level of theory in aqueous media was found to be 6.7 kcal/mol (Table 3).

The reaction shown in scheme 5 (Figure 4b) involves abstraction of the H atom attached to the C4 site by the OH radical. In this mechanism, PC5 is formed from RC5 through the transition state TS5. The BSSE-corrected Gibbs free energy barrier (ΔG_5^b) for scheme 5 at the MP2/AUG-cc-pVDZ level of theory in aqueous media was found to be 10.2 kcal/mol (Table 3). The reaction shown in scheme 6 (Figure 4c) involves abstraction of a hydrogen atom of the CH_3 group of NAC. In this case, the reaction starts from RC6, ends in the product complex PC6, and involves the transition state TS6. The BSSE-corrected Gibbs free energy barrier (ΔG_6^b) for scheme 6 at the MP2/AUG-cc-pVDZ level of theory in aqueous media was found to be 6.7 kcal/mol (Table 3). Here we note that the rate constants for schemes 4 and 6 (Table 4) are somewhat different though the Gibbs free energy barriers in the two cases are the same (6.7 kcal/mol). This difference has arisen as the tunneling factors are different in the two cases. The calculated rate constants for hydrogen atom abstraction by an OH radical from the different sites of NAC follow the order S6 > C15 > C2 > C4 > O9 > N1 (Table 4). Thus, there are two other sites also, besides the thiol group, i.e., C15 and C2 in NAC, from where hydrogen abstraction by an OH radical would occur efficiently.

Isospin density surfaces of RC2, TS2, and PC2 of scheme 2 for the spin density value of 0.01 are shown in Figures 5a−c, respectively. In RC2, the spin density is almost fully localized on the oxygen atom (O21) of the OH radical and delocalized on O21, S6, and H8 atoms in TS2, while in PC2, it is almost fully localized on the S6 atom. We note that the spin density changes occur mainly at the atoms involved in the reaction. Thus, spin density distribution appears to be a good measure of reactivity of the sites of NAC and the OH radical. Electron density surfaces of RC2, TS2, and PC2 corresponding to the electron density value of 0.2e (e = electronic charge) are shown in Figure 5d−f. The value 0.2e was considered, as the electron density distribution features in RC2, TS2, and PC2 were best revealed at this value, particularly near the sulfur atom. No drastic change in the electron density value on the OH moiety or the SH group is found to occur in going from RC2 to TS2 to PC2. Further, electron density is delocalized on the whole of each of RC2, TS2, and PC2, except on the SH group, where it is much less. Thus, in the present case, electron density distribution appears to be a less sensitive measure of reactivity than spin density distribution.

4. Conclusions

The present study leads us to the following conclusions:

(i) The thiol group of NAC is mainly involved in the scavenging action for the OH radical. The abstraction of the hydrogen atom of the thiol group by an OH radical occurs with a low-barrier energy or barrierlessly and a high rate constant. Our theoretical results in this regard qualitatively agree with experimental observations.

(ii) The present calculations predict that the hydrogen atom attached to the α-carbon as well as the hydrogen atoms of the CH_3 group would be abstracted by an OH radical quite efficiently, though much less efficiently than the hydrogen atom of the thiol group. Therefore, these reactions can also contribute to the scavenging action of NAC for the OH radical to some extent.

(iii) The barrier energies and Gibbs free energy changes obtained using the BHandHLYP functional are much closer to those obtained by the MP2 method than those obtained by the B3LYP functional. Thus, the BHandHLYP functional appears to be significantly better than the B3LYP functional in the present context.

Acknowledgment. The authors are thankful to the University Grants Commission (New Delhi) and the Council of Scientific and Industrial Research (New Delhi) for financial support.

References and Notes

(1) Flora, S. D.; Izzotti, A.; D'Agostini, F.; Balansky, R. M. *Carcinogenesis* **2001**, *22*, 999.
(2) Wiseman, H.; Halliwell, B. *Biochem. J.* **1996**, *313*, 17.
(3) Aust, A. E.; Eveleigh, J. F. *Proc. Soc. Exp. Biol. Med.* **1999**, *222*, 246.
(4) Hussain, S. P.; Hofseth, L. J.; Harris, C. C. *Nat. Rev. Cancer* **2003**, *3*, 276.
(5) Yermilov, V.; Yosnie, Y.; Rubio, J.; Ohshima, H. *FEBS Lett.* **1996**, *399*, 67.
(6) Cadet, J.; Delatour, T.; Douki, T.; Gasparutto, D.; Pouget, J. P.; Sauvaigo, S. *Mutat. Res.* **1999**, *424*, 9.
(7) Kino, K.; Sugiyama, H. *Chem. Biol.* **2001**, *8*, 369.
(8) Bruner, S. D.; Norman, D. P. G.; Verdine, G. C. *Nature* **2000**, *403*, 859.
(9) White, B.; Smyth, M. R.; Stuart, J. D.; Rusling, J. F. *J. Am. Chem. Soc.* **2003**, *125*, 6604.
(10) Caporaso, N. J. *Natl. Cancer. Inst.* **2003**, *95*, 1263.
(11) Ramakrishnan, N.; Kalinich, J. F.; McClain, D. E. *Biochem. Pharmacol.* **1996**, *51*, 1443.
(12) Jena, N. R.; Mishra, P. C. *J. Phys. Chem. B* **2005**, *109*, 14205.
(13) Vaya, J.; Aviram, M. *Curr. Med. Chem. Immunol., Endocr. Metab. Agents* **2001**, *1*, 99.
(14) Tanaka, T.; Makita, H.; Ohnishi, M.; Mori, H.; Satoh, K.; Hara, A.; Sumida, T.; Fukutani, K.; Ogawa, H. *Cancer Res.* **1997**, *57*, 246.
(15) Shukla, M. K.; Mishra, P. C. *J. Mol. Struct.* **1996**, *377*, 247.
(16) McCall, M. R.; Frei, B. *Free Rad. Biol. Med.* **1999**, *26*, 1034.
(17) Kelly, G. S. *Altern. Med. Rev.* **1998**, *3*, 114.
(18) De Vries, N.; De Flora, S. J. *Cell Biochem. Suppl.* **1993**, *17*, 270.
(19) Shukla, M. K.; Mishra, P. C. *Spectrochim. Acta Part A* **1995**, *51*, 831.
(20) Balendiran, G. K.; Dabur, R.; Fraser, D. *Cell Biochem. Funct.* **2004**, *22*, 343.
(21) Kerksick, C.; Willoughby, D. J. *Int. Soc. Sport Nutr.* **2005**, *2*, 38.
(22) Hemat, R. A. S.; Hemat, R. *Urotext* **2003**.
(23) Nijmeijer, B. A.; Steenvoorden, D. P.; Beijersbergen Van Henegouwen, G. M.; Roza, L.; Vink, A. A. J. *Photochem. Photobiol. B: Biol.* **1998**, *44*, 225.
(24) Emonet-Piccardi, N.; Richard, M. J.; Ravanat, J. L.; Signorini, N.; Cadet, J.; Beani, J. C. *Free Rad. Res.* **1998**, *29*, 307.
(25) Firat, S.; Aricioglu, A.; Akmansu, M.; Kilinc, M.; Ozagul, C.; Firat, H. *Biochem. Arch.* **1999**, *15*, 117.
(26) Morley, N.; Curnow, A.; Salter, L.; Campbell, S.; Gould, D. J. *Photochem. Photobiol. B: Biol.* **2003**, *72*, 55.
(27) Ates, B.; Abraham, L.; Ercal, N. *Free Rad. Res.* **2008**, *42*, 372.
(28) Sober, H. A. *Handbook of Biochemistry*, 2nd ed.; Cleveland, OH, 1970.
(29) Aruoma, O. I.; Halliwell, B.; Hoey, B. M.; Butler, J. *Free Rad. Biol. Med.* **1989**, *6*, 593.
(30) Gillissen, A.; Nowak, D. *Respir. Med.* **1998**, *92*, 609.
(31) Vanderbist, F.; Maes, P.; Neve, J. *Arzneimittelforschung* **1996**, *46*, 783.
(32) Malins, D. C.; Hellstrom, K. E.; Anderson, K. M.; Johnson, P. M.; Vinson, M. A. *Proc. Natl. Acad. Sci. U.S.A.* **2002**, *99*, 5937.
(33) Ercal, N.; Oztezcan, S.; Hammond, T. C.; Matthews, R. H.; Spitz, D. R. *J. Chromatogr. B* **1996**, *685*, 329.
(34) Toussaint, B.; Pitti, C.; Streel, B.; Ceccato, A.; Hubert, P.; Crommen, J. *J. Chromatogr. B* **2000**, *896*, 191.
(35) Lee, C.; Yang, W.; Parr, R. G. *Phys. Rev. B* **1988**, *37*, 785.
(36) Becke, A. D. *J. Chem. Phys.* **1993**, *98*, 5648.
(37) Szori, M.; Fittschen, C.; Csizmadia, I. G.; Viskolcz, B. J. *Chem. Theor. Comput.* **2006**, *2*, 1575.
(38) Tiwari, S.; Shukla, P. K.; Mishra, P. C. *J. Mol. Model* **2008**, *14*, 631.
(39) Frisch, M. J.; Head-Gordon, M.; Pople, J. A. *Chem. Phys. Lett.* **1990**, *166*, 275.
(40) Møller, C.; Plesset, M. S. *Phys. Rev.* **1934**, *46*, 618.
(41) Miertus, S.; Scrocco, E.; Tomasi, J. *Chem. Phys.* **1981**, *55*, 117.
(42) Cossi, M.; Scalmani, G.; Rega, N.; Barone, V. *J. Chem. Phys.* **2002**, *117*, 43.
(43) Gonzalez, C.; Schlegel, H. B. *J. Chem. Phys.* **1989**, *90*, 2154.

(44) Boys, S. F.; Bernardi, F. *Mol. Phys.* **1970**, *19*, 553.
(45) Simon, S.; Duran, M.; Dannenberg, J. J. *J. Chem. Phys.* **1996**, *105*, 11024.
(46) Frisch, M. J.; Trucks, G. W.; Schlegel, H. B.; Scuseria, G. E.; Robb, M. A.; Cheeseman, J. R.; Zakrzewski, V. G.; Montgomery, J. A., Jr.; Stratmann, R. E.; Burant, J. C.; Dapprich, S.; Millam, J. M.; Daniels, A. D.; Kudin, K. N.; Strain, M. C.; Farkas, O.; Tomasi, J.; Barone, V.; Cossi, M.; Cammy, R.; Mennucci, B.; Pomelli, C.; Adamo, C.; Clifford, S.; Ochterski, J.; Petersson, G. A.; Ayala, P. Y.; Cui, Q.; Morokuma, K.; Rega, N.; Salvodar, P.; Dannenberg, J. J.; Malick, D. K.; Rabuck, A. D.; Raghavachari, K.; Foresman, J. B.; Cioslowski, J.; Ortiz, J. V.; Baboul, A. G.; Stefanov, B. B.; Liu, G.; Liashenko, A.; Piskorz, P.; Komaromi, I.; Gomperts, R.; Martin, R. L.; Fox, D. J.; Keith, T.; AlLaham, M. A.; Peng, C. Y.; Nanayakkara, A.; Challacombe, M.; Gill, P. M. W.; Johnson, B.; Chen, W.; Wong, M. W.; Andres, J. L.; Gonzalez, C.; HeadGordon, M.; Replogle, E. S.; Pople, J. A. *Gaussian 03*, Revision B.05; Gaussian, Inc.: Pittsburgh PA, 2003.
(47) Frisch, M. J.; Trucks, G. W.; Schlegel, H. B.; Scuseria, G. E.; Robb, M. A.; Cheeseman, J. R.; Zakrzewski, V. G.; Montgomery, J. A., Jr.; Stratmann, R. E.; Burant, J. C.; Dapprich, S.; Millam, J. M.; Daniels, A. D.; Kudin, K. N.; Strain, M. C.; Farkas, O.; Tomasi, J.; Barone, V.; Cossi, M.; Cammy, R.; Mennucci, B.; Pomelli, C.; Adamo, C.; Clifford, S. Ochterski, J.; Petersson, G. A.; Ayala, P. Y.; Cui, Q.; Morokuma, K.; Rega, N.; Salvodar, P.; Dannenberg, J. J.; Malick, D. K.; Rabuck, A. D.; Raghavachari, K.; Foresman, J. B.; Cioslowski, J.; Ortiz, J. V.; Baboul, A. G.; Stefanov, B. B.; Liu, G.; Liashenko, A.; Piskorz, P.; Komaromi, I.; Gomperts, R.; Martin, R. L.; Fox, D. J.; Keith, T.; AlLaham, M. A.; Peng, C. Y.; Nanayakkara, A.; Challacombe, M.; Gill, P. M. W.; Johnson, B.; Chen, W.; Wong, M. W.; Andres, J. L.; Gonzalez, C.; HeadGordon, M.; Replogle, E. S.; Pople, J. A. *Gaussian 98*, Revision A.11.2; Gaussian, Inc.: Pittsburgh PA, 2001.
(48) Frisch, A. E.; Dennington, R. D.; Keith, T. A.; Neilsen, A. B.; Holder, A. J. *GaussView*, Revision 3.09; Gaussian, Inc.: Pittsburgh PA, 2003.
(49) Laidler, K. J. *Chemical Kinetics*, 3rd ed.; Pearson Education (Singapore) Pte. Ltd.: Indian Branch, 482, F.I.E. Patparganj, Delhi 110092, India, 2004.
(50) Levine, I. N. *Quantum Chemistry*, 4th ed.; Prentice-Hall, Inc.: Englewood Cliffs, N.J., U.S.A., 1994.
(51) Ramalho, S. S.; Vilela, A. F. A.; Barreto, P. R. P.; Gargano, R. *Chem. Phys. Lett.* **2005**, *413*, 151.
(52) Carstensen, H. H.; Dean, A. M. *J. Phys. Chem. A* **2009**, *113*, 367.
(53) Henon, E.; Bohr, F. J. *Mol. Struct. (Theochem)* **2000**, *531*, 283.
(54) Bieri, M.; Burgi, T. *J. Phys. Chem. B* **2005**, *109*, 22476.
(55) Dobrowolski, J. C.; Rode, J. E.; Sadlej, J. J. *Mol. Struct. (Theochem)* **2007**, *810*, 129.
(56) Tiwari, S.; Mishra, P. C. *Spectrochim. Acta Part A* **2009**, *73*, 719.
(57) Tiwari, S.; Mishra, P. C.; Suhai, S. *Int. J. Quantum Chem.* **2008**, *108*, 1004.

JP903604S